EXAFS studies of FeMo-cofactor and MoFe protein: Direct evidence for the long-range Mo-Fe-Fe interaction and cyanide binding to the Mo in FeMo-cofactor

ARTICLE *in* JOURNAL OF THE AMERICAN CHEMICAL SOCIETY · APRIL 1994

Impact Factor: 12.11 · DOI: 10.1021/ja00085a022

8 AUTHORS, INCLUDING:

Andrea Di Cicco
University of Camerino
204 PUBLICATIONS **3,957** CITATIONS

SEE PROFILE

EXAFS Studies of FeMo-Cofactor and MoFe Protein: Direct Evidence for the Long-Range Mo-Fe-Fe Interaction and Cyanide Binding to the Mo in FeMo-Cofactor

Hongbin Isaac Liu,[1a] Adriano Filipponi,[1b] Narasaiah Gavini,[1c] Barbara K. Burgess,[1c] Britt Hedman,[1d] Andrea Di Cicco,[1e] Calogero R. Natoli,[1f] and Keith O. Hodgson*[,1a,d]

Contribution from the Department of Chemistry, Stanford University and Stanford Synchrotron Radiation Laboratory, Stanford California 94305, Dipartimento di Fisica, Università degli Studi dell'Aquila, Via Vetoio, 67010 Coppito, L'Aquila, Italy, Department of Molecular Biology and Biochemistry, University of California, Irvine, California 92717, Dipartimento di Matematica e Fisica, Università degli Studi di Camerino, Via Madonna delle Carceri, 62032 Camerino (MC), Italy, and INFN, Laboratori Nazionali di Frascati-C.P. 13, 00044 Frascati, Italy

Received September 27, 1993®

Abstract: The biological reduction of dinitrogen to ammonia by the nitrogenase system requires the MoFe protein, which contains two iron-molybdenum cofactors (FeMoco) and two Fe-S P-clusters, and the Fe protein, which is the electron donor in catalysis. The two FeMo-cofactors are the likely sites of substrate binding and reduction, and knowledge of their detailed structure and function is central to understanding the chemistry of this complex enzyme system. Recent crystal structure studies of the MoFe protein are providing remarkable details about the MoFe protein, but questions about the structure of isolated FeMoco and reactivity of the FeMoco site remain unanswered. We report herein a new series of Mo-K edge EXAFS studies of highly concentrated isolated FeMoco, isolated FeMoco plus CN^-, and the MoFe protein. Very high quality data has been obtained over a wide *k*-range through improved experimental techniques. In addition, new EXAFS analysis methodology (called GNXAS) based on multiple scattering formalism with further enhancements has been used to analyze the data. Several important results have emerged: for the first time a second shell of Fe atoms at ~5.1 Å from the Mo is clearly present in the EXAFS for ***both*** FeMoco and the MoFe protein. This provides direct evidence for the "intact" nature of extracted FeMoco and demonstrates the ability to detect and analyze such long-range absorber-scatter interactions. Second, the EXAFS results give very accurate metrical details of the FeMoco sites, and these differ from those of FeMoco from the X-ray crystal structure of the MoFe protein at its current level of refinement. Finally, using the GNXAS analysis method, it is shown that added CN^- coordinates to Mo in isolated FeMoco. These results further define accurate metrical details of FeMoco within and outside of the protein and provide the methodological basis for further investigations of chemical reactivity.

Introduction

The nitrogenase enzyme system catalyzes the biological reduction of dinitrogen to ammonia. The molybdenum nitrogenases consist of an MoFe protein, which contains two iron-molybdenum cofactors (FeMoco or M-cluster) and two Fe-S P-clusters, and an Fe protein, which is the electron donor in catalysis.[2] The two FeMocos, each of stoichiometry $Mo:Fe_7:S_9^{2-}$:homocitrate, are the likely sites of substrate binding and reduction.[3] FeMoco can be studied within the native protein or in an "isolated" form in *N*-methylformamide (NMF). There is substantial physical evidence suggesting that the two species are similar but not identical.[2,4]

Extended X-ray absorption fine structure (EXAFS) studies at the Mo K absorption edge provided the first definitive structural evidence that the Mo in the MoFe protein from *Clostridium pasteurianum* was a part of an unprecedented polynuclear cluster containing Fe and S.[5] Due to inadequate signal-to-noise in the data and the lack of suitable models for empirical parameters, only S and Fe could be unambiguously identified as Mo nearest neighbors. A comparative study of Mo K EXAFS from *Azotobacter vinelandii* MoFe protein with the FeMoco extracted from it indicated that the basic features of the Mo environment remained unchanged in isolated FeMoco.[6] Subsequently, second generation Mo-K edge and EXAFS experiments further defined the nature of this Mo-containing cluster and revealed the additional presence of low-Z ligands on Mo.[7] The Mo site was determined to have an approximately octahedral environment, occupying the corner of a $MoFe_3S_3$ moiety.[7] Fe K-edge EXAFS studies were also used to confirm the results obtained from the Mo K-edge studies for isolated FeMoco[8] and have also provided evidence for longer range interactions in FeMoco.[9]

Pioneering X-ray crystal structure studies have recently provided complete structural details about the MoFe protein for both *A. vinelandii*[10] and *C. pasteurianum*,[11] including the full structure of the FeMoco. The refinement of the structural model for FeMoco of resting state *A. vinelandii* MoFe protein at 2.2 Å

* Abstract published in *Advance ACS Abstracts,* February 15, 1994.

(1) (a) Stanford University. (b) Università degli Studi dell'Aquila. (c) University of California at Irvine. (d) Stanford Synchrotron Radiation Laboratory. (e) Università degli Studi di Camerino. (f) INFN.

(2) Burgess, B. K. *Chem. Rev.* **1990**, *90*, 1377-1406.

(3) (a) Shah, V. K.; Brill, W. J. *Proc. Natl. Acad. Sci. U.S.A.* **1977**, *74*, 3249-3253. (b) Hawkes, T. R.; McLean, P. A.; Smith, B. E. *Biochem. J.* **1984**, *217*, 317-321. (c) Scott, D. J.; May, H. D.; Newton, W. E.; Brigle, K. E.; Dean, D. R. *Nature (London)* **1990**, *343*, 188-190.

(4) Newton, W. E. In *Biological Nitrogen Fixation*; Stacey, G.; Burns, R. H., Evans, H. J., Eds.; Chapman & Hall: New York, 1992; pp 877-929.

(5) Cramer, S. P.; Hodgson, K. O.; Gillum, W. O.; Mortenson, L. E. *J. Am. Chem. Soc.* **1978**, *100*, 3398-3407.

(6) Cramer, S. P.; Gillum, W. O.; Hodgson, K. O.; Mortenson, L. E.; Stiefel, E. I.; Chisnell, J. R.; Brill, W. J.; Shah, V. K. *J. Am. Chem. Soc.* **1978**, *100*, 3814-3819.

(7) Conradson, S. D.; Burgess, B. K.; Newton, W. E.; Mortenson, L. E.; Hodgson, K. O. *J. Am. Chem. Soc.* **1987**, *109*, 7507-7515.

(8) Antonio, M. R.; Teo, B.-K.; Orme-Johnson, W. H.; Nelson, M. J.; Groh, S. E.; Lindahl, P. A.; Kauzlarich, S. M.; Averill, B. A. *J. Am. Chem. Soc.* **1982**, *104*, 4703-4705.

(9) (a) Arber, J. M.; Flood, A. C.; Garner, C. D.; Gormal, C. A.; Hasnain, S. S.; Smith, B. E. *Biochem. J.* **1988**, *252*, 421-425. (b) Chen, J.; Christiansen, J.; Tittsworth, R. C.; Hales, B. J.; George, S. J.; Coucouvanis, D.; Cramer, S. P. *J. Am. Chem. Soc.* **1993**, *115*, 5509-5515.

(10) (a) Kim, J.; Rees, D. C. *Science* **1992**, *257*, 1677-1681. (b) Chan, M. K.; Kim, J.; Rees, D. C. *Science* **1993**, *260*, 792-794.

0002-7863/94/1516-2418$04.50/0

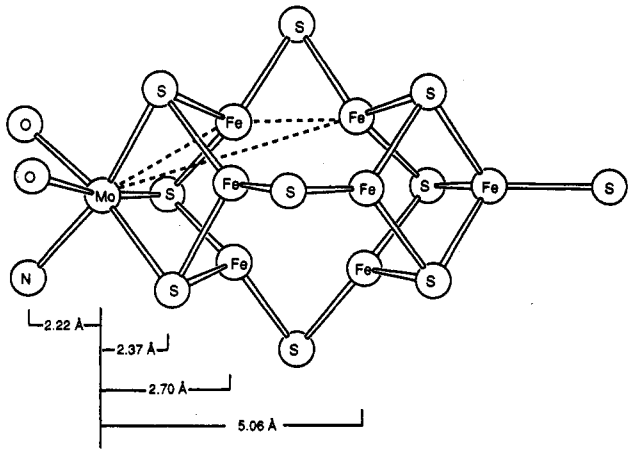

Figure 1. Structural model of the FeMoco site in nitrogenase determined from X-ray crystallographic studies (see text for additional description and references). The two subclusters, $MoFe_3S_3$ (left) and Fe_4S_3 (right), are bridged by three sulfides. Mo K-edge EXAFS analysis using multiple scattering (see text) provides accurate metrical details both within the $MoFe_3S_3$ subcluster and to the shell containing three Fe atoms in the Fe_4S_3 subcluster. The principal three-body multiple scattering pathway involving Mo is indicated by the dotted line. Shown below are the distances determined by EXAFS for the MoFe protein, including the long-range Mo···Fe interaction across the two subclusters.

provides structural details for the two cuboidal fragments, Fe_4S_3 and $MoFe_3S_3$, which according to the initial reports are bridged by two sulfides and a third ligand Y.[10] Further refinement indicates that the ligand Y is a third sulfide.[12] The only endogenous protein ligand that coordinates FeMoco through S is αCys275 which binds to a single Fe atom at the terminus of the Fe_4S_3 subcluster. The only additional ligands to FeMoco in the current model are αHis442 and homocitrate, both of which bind to Mo to complete its pseudooctahedral coordination. The $MoFe_3S_3$ subfragment was equivalent to that determined from the initial Mo K-edge EXAFS studies. A representation of the FeMoco structure is given in Figure 1.

Given the "resting-state" structure of the MoFe protein, a number of important problems remain to be addressed. There is still little experimental evidence that implicates Mo in any reactions of nitrogenase or in fact directly identifies the site(s) and nature of substrate interaction.[2] Indirect evidence for substrate binding to the MoFe protein has come from the observation that the $S = {}^3/_2$ EPR signal is pH-dependent and that the pK_a of this signal is shifted in the presence of C_2H_2.[13,14] A transient EPR signal, seen during turnover in the presence of C_2H_2, has also been interpreted as evidence for interaction with the FeMoco.[15] The substrates CN^- and CH_3NC are interesting because besides being reduced by six electrons, they also bind to nitrogenase in nonproductive modes that prevent substrate reduction but not ATP hydrolysis.[2] Mo K-edge EXAFS studies of dithionite-reduced MoFe protein in the presence of CN^- and CH_3NC showed no detectable differences, suggesting Mo was not involved at least under the set of concentrations and experimental conditions used for those studies.[16]

Lack of observed substrate binding could reflect the fact that the fully reduced form of the protein (which is active in turnover) may be required or that the binding sites become accessible only during turnover conditions. For these reasons, and indeed because of the broad interest in the chemistry and synthesis of FeMoco itself, study of the interaction of substrates and other exogenous ligands with isolated FeMoco are relevant. Direct evidence for interaction of CN^- with isolated FeMoco first came from observation that the $S = {}^3/_2$ signal was altered upon addition of CN^-,[17] and the data were interpreted in terms of two CN^- binding sites. NMR studies using ^{19}F-labeled thiolates as reporter ligands demonstrated that both CN^- and CH_3NC bind to isolated FeMoco without displacing bound thiolate ligand.[16] More recently, ligand-based Se-K EXAFS studies have provided direct evidence that benzeneselenol (and by analogy thiol) bind to Fe (and not Mo) for isolated FeMoco.[18]

Further insight into the structure of isolated FeMoco, how it relates to the structure found within the MoFe protein, and how it reacts with substrates are needed. While EPR and early EXAFS studies referenced above suggested that at least the $MoFe_3S_3$ subfragment of FeMoco is retained upon removal from the protein, the lack of a crystal structure of isolated FeMoco has precluded comparison to the form found within the protein. Recent improvements in experimental methodology and analysis of EXAFS data have provided an opportunity to obtain additional insights into these questions of structure and reactivity. Significant improvements in the quality and available energy range (which correlates with resolution) of EXAFS data for very dilute metalloproteins have come through the use of high-energy-resolution array detectors and measurements at 10 K coupled with improvements in beam stability and higher currents now being provided by the synchrotron facilities. In addition, more sophisticated analysis of EXAFS data utilizing full curved-wave, multiple scattering analysis has become feasible.[19] EXAFS can also provide significantly more accurate near-neighbor coordination distances than available from medium-resolution (2–2.5 Å) protein structures which typically have esds in the range of a few tenths of an Å.[20]

We have recently used a new integrated set of programs called GNXAS[21] (which are based upon such a full curved-wave multiple scattering formalism and use Hedin–Lundqvist complex exchange and correlation potential) to investigate the accuracy of EXAFS determination in a polynuclear Mo–Fe–S cluster of known structure which has several structural features in common with FeMoco.[22] The ability of the GNXAS method to investigate long-range order in such polynuclear heterometal clusters was evaluated, near neighbor distances were determined to typically ±0.015 Å, and heavy atoms in shells out to around 5 Å from the Mo could be quantified.[22] Multiple scattering analysis also provides reasonably accurate angular information from three-

(11) (a) Bolin, J. T.; Ronco, A. E.; Morgan, T. V.; Mortenson, L. E.; Xuong, N.-H. *Proc. Natl. Acad. Sci. U.S.A.* **1993**, *90*, 1078–1082. (b) Kim, J.; Woo, D.; Rees, D. C. *Biochem.* **1993**, *32*, 7104–7115.

(12) Rees, D. C., personal communication.

(13) (a) Smith, B. E.; Lowe, D. J.; Bray, R. C. *Biochem. J.* **1973**, *135*, 331–341. (b) Euler, W. B.; Martinsen, J.; McDonald, J. W.; Watt, G. D.; Wang, Z.-C. *Biochem.* **1984**, *23*, 3021–3024.

(14) Smith, B. E. in *Nitrogen Fixation: The Chemical-Biochemical-Genetic Interface*; Müller, A., Newton, W. E., Eds.; Plenum Press: New York, 1983; p 23–62.

(15) Hawkes, T. R.; Lowe, D. J.; Smith, B. E. *Biochem. J.* **1983**, *211*, 495–497.

(16) Conradson, S. D.; Burgess, B. K.; Vaughn, S. A.; Roe, A. L.; Hedman, B.; Hodgson, K. O.; Holm, R. H. *J. Biol. Chem.* **1989**, *264*, 15967–15974.

(17) Smith, B. E.; Bishop, P. E.; Dixon, R. A.; Eady, R. R.; Filler, W. A.; Lowe, D. J.; Richards, A. J. M.; Thomson, A. J.; Thorneley, R. N. F.; Postgate, J. R. In *Nitrogen Fixation Research Progress*; Evans, H. J., Bottomley, P. J., Newton, W. E., Eds.; Martinus Nijhoff: Dordrecht, 1985; pp 597–603.

(18) Conradson, S. D.; Burgess, B. K.; Newton, W. E.; Di Cicco, A.; Filipponi, A.; Wu, Z. Y.; Natoli, C. R.; Hedman, B.; Hodgson, K. O. *Proc. Natl. Acad. Sci. U.S.A.*, in press.

(19) (a) Gurman, S. J.; Binsted, N.; Ross, I. *J. Phys. C* **1986**, *19*, 1845–1861. (b) Rehr, J. J.; Albers, R. C. *Phys. Rev. B* **1990**, *41*, 8139–8149. (c) Mustre de Leon, J.; Rehr, J. J.; Zabinsky, S. I.; Albers, R. C. *Phys. Rev. B* **1991**, *44*, 4146–4156. (d) Filipponi, A.; Di Cicco, A.; Tyson, T. A.; Natoli, C. R. *Solid State Commun.* **1991**, *78*, 265–268.

(20) For medium resolution X-ray crystal structure analyses, esds on metal clusters should be in the range of a few tenths of Å for proteins such as the MoFe protein. EXAFS analysis has been used before to provide more accurate structure determination of metal sites than were available from crystallographic refinement. A useful discussion of this can be found: Shulman, R. G.; Eisenberger, P.; Teo, B. K.; Kincaid, B. M.; Brown, G. S. *J. Mol. Biol.* **1978**, *124*, 305–321.

(21) The GNXAS acronym derives from g_n (the n-body distribution function) and XAS (X-ray absorption spectroscopy).

(22) Norlander, E.; Lee, S. C.; Cen, W.; Wu, Z. Y.; Natoli, C. R.; Di Cicco, A.; Filipponi, A.; Hedman, B.; Hodgson, K. O.; Holm, R. H. *J. Am. Chem. Soc.* **1993**, *115*, 5549–5558.

body pathways whose amplitude is significant (such as selected Mo–Fe–Fe pathways in clusters). Another case is that of linear (or near linear) coordination of a diatomic molecule such as CN^- or CO, where the strongly enhanced forward scattering (the so-called intervening atom focussing effect[23]) can be accurately analyzed providing enhanced sensitivity toward detection and structural characterization of such ligands bound to metals.

The studies described herein utilize the improved EXAFS data quality achievable and the more advanced multiple scattering EXAFS analysis using GNXAS for structural studies of isolated FeMoco with and without added CN^- and of the dithionite-reduced MoFe protein. The results give quantitative information about long-range order and accurate metrical details of FeMoco within and outside of the protein. A comparison with the structure of FeMoco at the 2.2 Å level of crystallographic refinement is made. Studies of CN^- binding to isolated FeMoco provide insights into the chemical reactivity of Mo.

Experimental Section

Sample Preparation and Handling. *A. vinelandii* MoFe protein (108 mg/mL) and FeMoco (3.6 mM in Mo) were isolated, concentrated, and assayed according to published methods.[24] Activity for all samples studied was found to be in the range of 240–260 nmol C_2H_4 formed/min/ng atom Mo and remained within 10% of this value after the EXAFS experiments. All samples contained an excess of dithionite to ensure that the semireduced state of both protein and FeMoco was maintained. CN^- was added as a 365 mM solution of NaCN in NMF giving a ratio of 1:5 Mo:CN^-. All sample manipulation was performed in a Vacuum Atmospheres inert (N_2) dry glovebox. The samples were loaded into sealable cells under anaerobic conditions, frozen immediately upon removal from the box, and maintained at dry ice temperature or lower throughout.

Model compounds used to obtain empirical phase and amplitudes were synthesized according to the literature methods: $Mo(SC_6H_4)_3$,[25] $Mo(acac)_3$,[26] $(Et_4N)_3[Mo_2Fe_6S_8(OCH_3)_3(SPh)_6]$,[27] and $(n\text{-}Bu_4N)_3[Mo_2Fe_6S_8(SPh)_9]$.[28] The solid samples were ground to a fine powder and diluted with BN in the glovebox. The mixture was pressed into a pellet and sealed between 63.5 μm Mylar windows in a 1-mm Al spacer. The samples were frozen in liquid nitrogen immediately upon removal from the glovebox and maintained at this or lower temperatures throughout.

Collection and Reduction of X-ray Absorption Spectroscopy Data. Mo K-edge X-ray absorption spectra were collected at the Stanford Synchrotron Radiation Laboratory on unfocussed multipole wiggler beam lines 10–2 and 7–3 under dedicated ring conditions (3.0 GeV, 50–100 mA) using a Si(220) double-crystal monochromator. The spectra were all recorded at sample temperatures of 10 K, maintained using an Oxford Instruments CF1208 liquid He cryostat. Internal energy calibration was performed assigning the first inflection point of Mo foil to 20 003.9 eV. The Mo model compounds were measured in transmission mode and the protein data as fluorescence spectra (using a 13-element Ge array detector[29] for the protein, a Kr-filled ionization chamber fluorescence detector[30] equipped with Zr filter and Soller slits for FeMoco). The data represent averages of multiple scans (typically 15–20), with data collection and reduction as described previously in detail.[31]

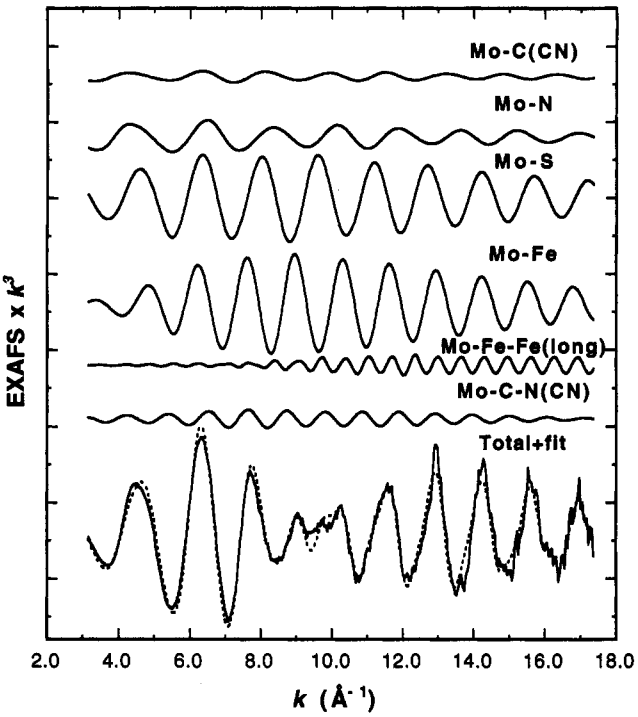

Figure 2. Individual contributions to the EXAFS signal in the final fit for Mo K-edge data for FeMoco + CN^-. The total signal is also shown (···) compared with the experimental signal (—) (the ordinate scale is 10 indicated between two consecutive large marks). The signals from N(1)—the distant N on CN^-—is seen to make a significant contribution because of the linear focusing effect (see also Figures 1 and 5 for comparison of amplitudes in FTs). The Mo–Fe–Fe(long) is the total signal for the long Fe shell around 5 Å from Mo. This signal is comprised of about 60% single and 40% multiple scattering contributions and accounts well for the asymmetric feature in the FT around R = 4.8 Å (see Figure 3 and text). Fits to isolated FeMoco and MoFe protein (data not shown) were of quality comparable to that shown here.

Analysis of X-ray Absorption Spectroscopy Data. The principal method of EXAFS data analysis utilized the integrated GNXAS[19d,32] method with theoretical phase and amplitude parameters. For comparison, the more conventional nonlinear least-squares curve-fitting empirical approach[33] was also used. For the empirical approach, phase and amplitude parameters were derived as described in ref 33 using model data of Mo-$(SC_6H_4)_3$, $Mo(acac)_3$, $(Et_4N)_3[Mo_2Fe_6S_8(OCH_3)_3(SPh)_6]$, and $(n\text{-}Bu_4N)_3[Mo_2Fe_6S_8(SPh)_9]$ for Mo–S, –O, and –Fe parameters, respectively. In the empirical fits, the coordination number and the Mo-scatterer distances were varied while the Debye–Waller factor was kept fixed at the extracted values.

GNXAS provides for *ab initio* modeling of EXAFS spectra including multiple-scattering pathways and proper treatment of correlated Debye–Waller factors.[19d] The application of this method to polynuclear Mo–Fe–S clusters of known structure establishes the methodology utilized herein.[22] The specific approach using GNXAS to analyze the EXAFS data herein is the same as that described in ref 22 where definitions of the least-squares residual R and other parameters are given. Structural parameters varied for each shell were R (distance) and σ^2

(23) (a) Teo, B.-K. *J. Am. Chem. Soc.* **1981**, *103*, 3990–4001. (b) Co, M. S.; Hendrickson, W. A.; Hodgson, K. O.; Doniach, S. *J. Am. Chem. Soc.* **1983**, *105*, 1144–1150.
(24) Burgess, B. K.; Jacobs, D. B.; Stiefel, E. I. *Biochem. Biophys. Acta* **1980**, *614*, 196–209.
(25) Cowie, M.; Bennett, M. *Inorg. Chem.* **1976**, *15*, 1584–1589.
(26) Raston, C. L.; White, A. H. *Aust. J. Chem.* **1979**, *32*, 507–512.
(27) Christou, G.; Garner, C. D. *J. Chem. Soc., Dalton Trans.* **1980**, 2354–2362.
(28) Wolff, T. E.; Berg, J. M.; Hodgson, K. O.; Frankel, R. B.; Holm, R. H. *J. Am. Chem. Soc.* **1979**, *101*, 4140–4150.
(29) Cramer, S. P.; Tench, O.; Yocum, M.; George, G. N. *Nucl. Instr. Meth.* **1988**, *A266*, 586–591.
(30) (a) Stern, E. A.; Heald, S. M. *Rev. Sci. Instrum.* **1979**, *50*, 1579–1582. (b) Lytle, F. W.; Greegor, R. B.; Sandstrom, D. R.; Marques, E. C.; Wong, J.; Spiro, C. L.; Huffman, G. P.; Huggins, F. E. *Nucl. Instr. Meth.* **1984**, *226*, 542–548.
(31) DeWitt, J. G.; Bentsen, J. G.; Rosenzweig, A. C.; Hedman, B.; Green, J.; Pilkington, S.; Papaefthymiou, G. C.; Dalton, H.; Hodgson, K. O.; Lippard, S. J. *J. Am. Chem. Soc.* **1991**, *113*, 9219–9235.
(32) Filipponi, A.; Di Cicco, A. *Synch. Rad. News* **1993**, *6*, 13–19.
(33) (a) Cramer, S. P.; Hodgson, K. O.; Stiefel, E. I.; Newton, W. E. *J. Am. Chem. Soc.* **1978**, *100*, 2748–2761. (b) Cramer, S. P.; Hodgson K. O. *Prog. Inorg. Chem.* **1979**, 25, 1–39. (c) Scott, R. A. *Methods Enzymol.* **1985**, *117*, 414–459.

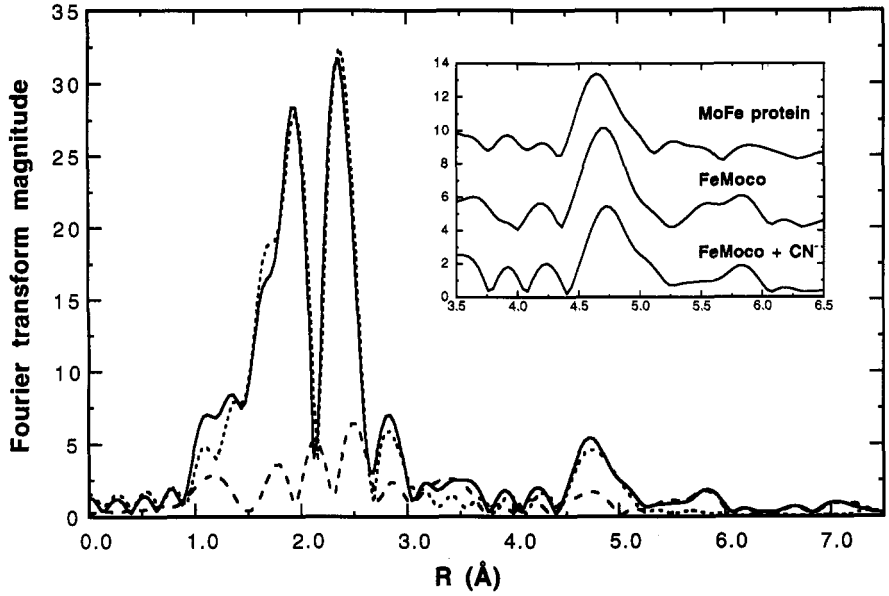

Figure 3. Fourier transforms of the Mo K-edge EXAFS (k-range 3.2–17 Å^{-1}) for FeMoco + CN$^-$ data. Transform of experimental data (—) is compared with that of the best theoretical fit (···), and the FT of the EXAFS residual is shown as (– –). The feature at R = 2.9 Å contains a significant contribution from the CN$^-$ second shell which ***is not well fit*** when the N of CN$^-$ is not included. The inset shows the region expanded around R = 4.8 Å for FeMoco + CN$^-$, MoFe protein, and isolated FeMoco. Note the presence in all three cases of the distinct asymmetric peak between 4.5 and 5 Å which derives from single + multiple scattering Mo–Fe (long), the analysis of which is discussed in the text. The magnitude and shape of the feature is best fit if multiple scattering signals (the primary ones being Mo–Fe–Fe(long), the dotted pathway shown in Figure 1) are included.

(the variance of R, which enters into the expression of the Debye–Waller factor, $e^{-2k^2\sigma^2}$, for a two-body signal) for single scattering and R1, R2, and θ with the respective bond and angle variances treated in a correlation matrix for multiple scattering. S_o^2 was fixed to 0.97, a value determined from fitting a number of Mo-containing clusters of known structure. Systematic errors are larger than statistical errors in this analysis as also discussed in more detail in ref 22. From the variances seen between GNXAS analysis of Mo–Fe–S clusters and crystallographic structure, esds from the EXAFS refinements are estimated to be ±0.015 Å for shells within about 3 Å of the Mo, ±0.03 Å for shells between 3 and 4 Å, and ±0.05 Å for further shells.[22]

Results and Discussion

Qualitative Analysis and Comparisons. EXAFS data and Fourier transforms for the isolated FeMoco + CN$^-$ sample are shown in Figures 2 and 3. The EXAFS data are of very high quality and signal-to-noise, the EXAFS modulations extending to beyond k = 17 Å^{-1} (see Figure 2, bottom). The very low, smooth signal above 6 Å in the Fourier transform (FT) also directly reflects the low noise level (Figure 3). The other two data sets (MoFe protein and isolated FeMoco) have very comparable signal-to-noise (data not shown). As is well-known from earlier studies (see Introduction), the dominant features in the FTs of Mo K-EXAFS for FeMoco and MoFe protein samples are the two features above and below 2 Å (note that these FT distances are ***not*** corrected for the phase shifts and thus underrepresent the true distances by about 0.3–0.4 Å). These two FT peaks derive from the Mo–S and Mo–Fe interactions within the $MoFe_3S_3$ subcluster. Not well resolved is a low-R shoulder on the peak below 2 Å which is from the low-Z ligands to Mo (external to the cluster).

The FTs for all three samples show unambiguous signals that contribute well above background beyond the range of those expected from the $MoFe_3S_3$ subcluster (that is at distances above ~3 Å). Most significant is the higher R, asymmetric peak at around 4.75 Å observed in all FTs of FeMoco and MoFe protein spectra reported herein (see inset, Figure 3). Based on the FeMoco crystallographic model (see Figure 1), this peak would likely derive from long-range Mo-Fe, referred to later as Fe(long), and/or Mo-S (in the bridge between the two subclusters) interactions. It is important to note that the very close similarities between FeMoco and MoFe protein in this region of the FT (Figure 3, insert) demonstrate that the *long-range order in the FeMoco cluster is preserved* when FeMoco is extracted into NMF. There is also a feature around 6 Å (Figure 3) which could derive from the next shell of S beyond the Fe(long) (that is the S shell in the Fe_4S_3 subcluster), but analysis of this will be the subject of future investigations.

An indirect indication of CN$^-$ interaction with Mo in isolated FeMoco is seen from the Mo-K X-ray absorption edges. As discussed in ref 5, Mo-K edges are sensitive to changes in oxidation state, site symmetry, and ligation of the Mo atom. Figure 4 compares the edges of FeMoco and FeMoco + CN$^-$. A small, but entirely reproducible difference is seen (Figure 4) upon addition of CN$^-$. Analysis of this feature has not been undertaken, but it may likely result from the low-energy multiple scattering resonances that could occur from binding of a diatomic like CN$^-$. Other explanations are possible, including interactions at other locations of FeMoco which indirectly perturb the electronic environment of the Mo. More direct evidence for ligation of CN$^-$ to Mo is provided by inspection of the FTs of the EXAFS data (Figure 5). For the FeMoco sample with CN$^-$ added, a feature at ~2.9 Å appears (indicated by the arrow), which has more than double the amplitude of that seen in spectra without CN$^-$. This feature occurs in a region expected to reflect multiple-scattering from the more distant N on CN$^-$, but this can only be verified by quantitative analysis (see below). We note that very similar observations of reproducible edge and Fourier transform changes have also been observed in preliminary data for samples of FeMoco + CN$^-$ + thiolate. This work is part of an ongoing, more in-depth study of FeMoco reactivity.[34]

(34) Earlier published studies from our laboratories (ref 16) concerned NMR and EXAFS studies of substrate interactions with the MoFe protein and isolated FeMoco. This study showed data (Figure 3.B, page 15973) for FeMoco, FeMoco + CH_3NC, MoFe protein, MoFe protein + CH_3NC, and MoFe protein + CN$^-$. No data were reported, nor were any measured for FeMoco + CN$^-$. The issue is confused in the paper by sentences which are ambiguous as to which samples were actually measured with which inhibitors. At the poorer level of energy resolution and S/N with the edge and EXAFS data for ***MoFe protein + CN$^-$***, no evidence for interaction could be seen. The protein studies, together with additional ligand-binding studies to isolated FeMoco are a subject of ongoing investigation using the improved experimental and analysis methodologies described in this paper.

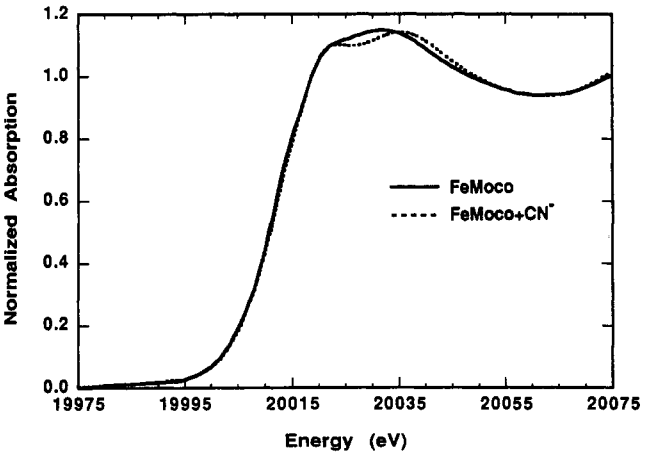

Figure 4. Comparison of Mo K X-ray absorption edges for isolated FeMoco with and without CN^-. A small but reproducible change is seen upon the addition of CN^- in the near-edge part of the spectrum. Mo K-edges are generally insensitive to electronic/geometric changes because of broadening due to core-hole lifetime effects and monochromator resolution, and this observed effect is surprisingly large. The observed change cannot be directly interpreted as CN^- ligation to Mo, only that there is an interaction occurring with FeMoco in some way that perturbs the Mo site. However, the edge data is consistent with evidence of CN^- interaction from other physical studies and with the EXAFS analysis of these samples (see text).

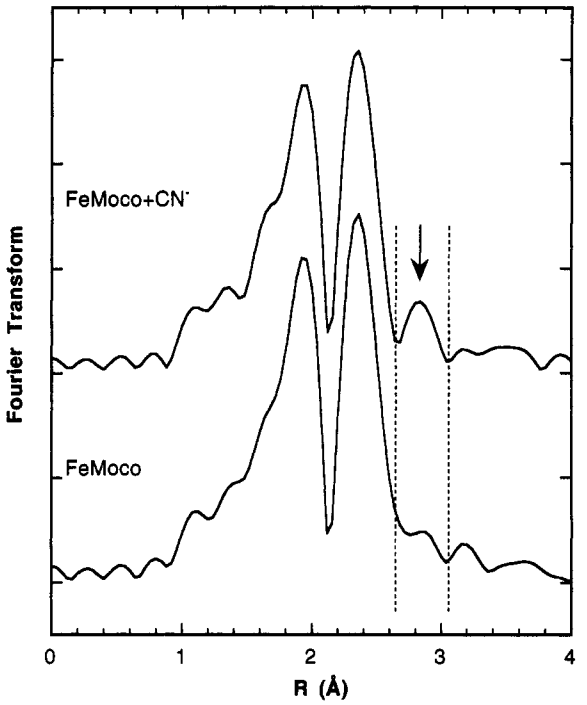

Figure 5. Fourier transforms of Mo K EXAFS data for isolated FeMoco and isolated FeMoco + CN^-. The FT for FeMoco + CN^- is the same as that shown in Figure 3, but expanded over the R-range 0–4 Å (the ordinate scale is 10 between two consecutive marks). The feature at R = 2.9 Å (see arrow) appears well above noise upon the addition of CN^-. This contribution is from the CN^- second shell, and the feature is not well fit when the N of CN^- is not included (see text for discussion and quantitative analysis).

Quantitative EXAFS Analysis. Quantitative analysis was done using curve fitting techniques. For reasons elaborated elsewhere, the GNXAS approach is expected to give the most reliable bond distances and coordination numbers for these clusters, particularly for the more distant shells.[22] However, the empirical analysis approach was also applied for further verification and comparison, even though it is limited to single-scattering. GNXAS was first used to fit the EXAFS contributions from the three shells of the $MoFe_3S_3$ subcluster. The fits were done over the range k = 3.2–17 $Å^{-1}$ using fixed coordination numbers and variable Debye–Waller factors. For the first shell low-Z ligands external to the cluster, equivalent fits could be obtained with either O or N. The results were for isolated FeMoco—3 O/N @ 2.19 Å, 3 S @ 2.37 Å, and 3 Fe @ 2.72 Å; for MoFe protein—3 O/N @ 2.22 Å, 3 S @ 2.37 Å, and 3 Fe @ 2.70 Å. Fits were of excellent quality (all comparable or better than that shown in Figure 2). Errors in distances are estimated to be better than ±0.015 Å based on variances in EXAFS and crystallographic analysis.[22] In all GNXAS fits the bond variances were in the range of 1–4 × 10^{-3} $Å^2$ with one exception, as discussed below. By comparison, Mo–S and Mo-Fe distances derived from GNXAS fits were all within 0.02 Å of the values determined using empirically derived phases and amplitudes for the same data sets, all of which are very similar to previously published results. The distances determined for the $MoFe_3S_3$ subcluster are all very similar to values previously published in the literature.[6,7,35] It is also worth noting that earlier published EXAFS[6,7] were best fit by an additional S-atom in MoFe protein compared to FeMoco. Using GNXAS analysis and the higher quality data described herein, it was also found that the quality of the fit was slightly improved (R decreasing from 9.49 × 10^{-7} to 7.40 × 10^{-7}) if an extra S atom is added to replace one N(or O) in the first shell of Mo, at a longer distance of about 2.5 Å. However, there is no apparent structural feature in the current crystallographic model that would enable such an effect to be observed. This effect is being further investigated on other FeMoco and MoFe protein samples.

A new, significant result is the analysis of the distinct features in EXAFS and FTs which derive from distances between the two subclusters, reflecting longer range order from Mo. Fitting of these features in the R = 4.3–5.3 Å range (Figure 3, insert) was first done with empirical phase and amplitude parameters. It was not possible to obtain a satisfactory fit of the 4.75 Å FT feature with a single shell (as would be clear from its asymmetry). It was clear, however, that Mo–Fe single scattering was an essential component for any reasonable fit to both isolated FeMoco and MoFe protein samples in this region of the spectrum. The empirical fits gave 2–3 Fe @ ~5.1 Å from Mo. More detailed analysis was done using multiple scattering GNXAS analysis. As expected, the main components to the 4.75 Å FT peak were found to be a long Mo–Fe(long) single scattering interaction combined with a Mo–Fe(short)–Fe(long) three-body multiple scattering pathway (shown by dotted lines in Figure 1). The Mo–Fe(long) contribution was determined to be 3 Fe @ 5.11 Å and @ 5.06 Å for isolated FeMoco and MoFe protein, respectively. The Mo–Fe(short)–Fe(long) bond angle was found to be 152° (FeMoco) and 153° (MoFe protein). These numbers compare with a range of Mo–Fe(long) distances and angles of 5.19–5.33 Å and 147–157° from the 2.2 Å refinement of the *A. vinelandii* protein crystal structure. It is worthwhile to note that both single and multiple scattering contributions were required to obtain a good fit (see Figure 6 for the fit to the FT for the MoFe protein). Careful inspection of other multiple-scattering pathways including Mo–S–Fe within the $MoFe_3S_3$ subcluster and Mo–Fe(short)–S(subcluster bridge) revealed quite small contributions that were not statistically significant. While sensible single + multiple scattering fits were possible (giving reasonable distances and angles) for the Mo–S(subcluster bridge), statistical significance (as judged by improvement to the quality of fit) was not adequate to justify their inclusion.

Given the very good results in fitting isolated FeMoco EXAFS using GNXAS, the same approach was used to study interaction of CN^- added to FeMoco solutions. For the FeMoco + CN^- fit, it was found that the 3 N(or O), 3 S, and 3 Fe single scattering signals did not fully explain the EXAFS, especially in the region

(35) Flank, A. M.; Weininger, M.; Mortenson, L. E.; Cramer, S. P. *J. Am. Chem. Soc.* **1986**, *108*, 1049–1055.

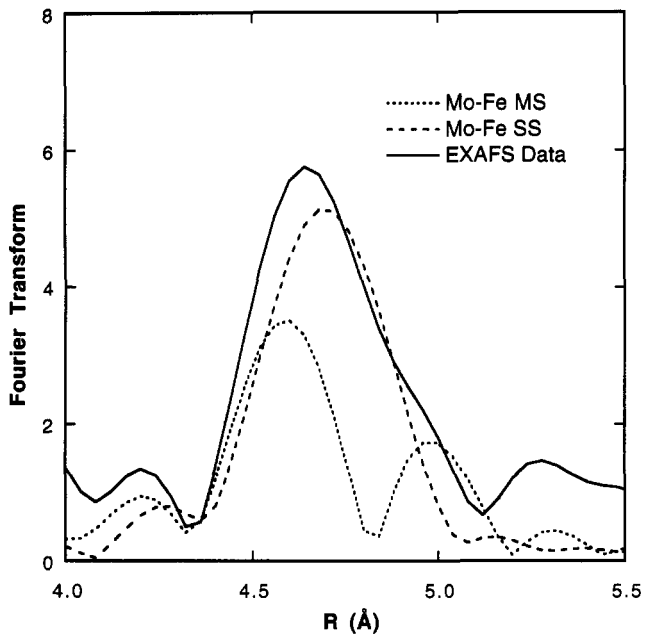

Figure 6. Expanded region (R = 4.0–5.5 Å) of the Fourier transform for MoFe protein EXAFS data which includes the contribution from the Mo–Fe (long) signal. The experimental FT (—) is compared with the single-scattering (– –) and total multiple-scattering (···) contributions from the best GNXAS fit. While the distance is relatively accurately determined by single-scattering, the asymmetry in the peak at longer R requires more than one frequency component as is clearly seen in the figure. The best GNXAS fits include about 60% single and 40% multiple scattering for this pathway (the pathway is shown as a dotted line, Figure 1). Distances and angles determined by the GNXAS analysis are discussed in the text, but the presence of the Mo–Fe(long) contribution is unambiguous. Very similar results (not shown) were observed for fits to isolated FeMoco and isolated FeMoco + CN^- data.

of the FT around 2.9 Å (Figures 1 and 5). An Mo–C single scattering and three-body multiple scattering contribution from a linear C–N interaction in CN^- were needed to obtain a good fit. The best fit to FeMoco + CN^- were for Mo coordinated to C and 2 O/N in the first shell. A Mo–C distance of 2.17 Å, a C–N distance of 1.15 Å, and a Mo–C–N angle of 180° (giving a Mo–N distance of 3.32 Å) were found, and the residual value for the fit decreased from 7.83×10^{-8} to 5.19×10^{-8} when comparing the same data fit with 3 O/N in the first shell. The other distances in the cluster remained essentially unchanged from isolated FeMoco—3 S @ 2.36 Å, 3 Fe @ 2.71 Å, and 3 Fe(long) @ 5.10 Å. The selected individual components contributing to this fit and the overall fit compared to the data are shown in Figure 2. The FT of the fit compared to the data and the FT of the residual are shown in Figure 3.

Comparison of Isolated FeMoco and MoFe Protein EXAFS with Crystallographic Results. The Mo–S and Mo–Fe distances determined from the EXAFS analysis described herein are slightly different than those of the *A. vinelandii* crystal structure model at 2.2 Å resolution.[12] For the two independent molecules of FeMoco in the MoFe protein, distances crystallographically determined for Mo–S range 2.42–2.50 Å, for Mo–Fe 2.84–2.98 Å, and for Mo–Fe(long) 5.19–5.33 Å. The EXAFS distances, for which the esds are significantly lower (see discussion of EXAFS errors in Experimental Section), are an average of about 0.2 Å shorter for the distances within the $MoFe_3S_3$ subcluster and at the low end of the range observed for the Mo–Fe(long) interaction. The Debye–Waller factors determined from the EXAFS fits fall within rather narrow ranges that are similar to those seen for fits of a regular Mo–Fe–S cluster of known structure.[22] An interesting exception is the bond variance factor for the Mo–Fe(short)–S(subcluster bridge) contribution of 4.9×10^{-3} Å^2 (for the single scattering pathway) which is about twice that found for the Mo–Fe(long) contribution, indicating high thermal motion or static disorder. As mentioned above, there has been some doubt as to the exact nature of the third ligand bridging the two subclusters, though S now seems to be the best atom. It might be noted that the Mo-bridging atom distances in the crystal structure are in the range of 4.6–5.1 Å and that a distribution in the bridge distances would be reflected in the EXAFS analysis. However, overall the EXAFS results indicate a more symmetric structure than seen in the crystallographic structure at the current level of resolution (that is having less variation of distances within each given shell).

Summary. EXAFS analysis using theoretical parameters and multiple scattering with very high quality data for isolated FeMoco and the MoFe protein has reconfirmed previous first shell Mo–N(O), Mo–S, and Mo–Fe bond distances to Mo and within the $MoFe_3S_3$ subcluster. A long-range ~5.1 Å Mo–Fe interaction is clearly seen which contributes to the EXAFS as both single and multiple scattering contributions for both MoFe protein and isolated FeMoco. The slightly longer distances in FeMoco compared to MoFe protein suggest a slight relaxation of the cluster structure upon removal from the protein matrix. The high-resolution EXAFS results are clearly complementary to protein X-ray crystallography in that they provide very accurate bond distances (and in certain circumstances angles) and enable study under solution conditions where interaction with inhibitors and substrates can be most readily probed. The work further demonstrates the sensitivity to small molecule ligation even in complex clusters when multiple scattering effects enhance the visibility of binuclear ligands through linear or near-linear coordination. This GNXAS EXAFS analysis has shown that Mo in isolated FeMoco is a binding site for CN^-. These results provide the basis for further investigations of substrates and inhibitors with different states of the MoFe protein and isolated FeMoco.

Acknowledgment. We thank Prof. Douglas C. Rees, California Institute of Technology, for providing crystal structure coordinates for the *A. vinelandii* MoFe protein prior to publication. This research was supported by NSF CHE-91-21576 and NIH RR-01209 (to K.O.H) and NIH GM-43144 (to B.K.B.). X-ray absorption data were collected at the Stanford Synchrotron Radiation Laboratory (SSRL), which is supported by the U.S. Department of Energy, Office of Basic Energy Sciences, Divisions of Chemical and Materials Sciences. SSRL is also supported by the National Institutes of Health, Biomedical Research Technology Program, and by the U.S. Department of Energy, Office of Health and Environmental Research.